Flooding transition in the topography of toppling surfaces of stochastic and rotational sandpile models

J. A. Ahmed and S. B. Santra*
Department of Physics, Indian Institute of Technology Guwahati, Guwahati-781039, Assam, India
(Received 21 October 2011; published 9 March 2012)

A continuous phase transition occurs in the topography of toppling surfaces of stochastic and rotational sandpile models when they are flooded with liquid, say water. The toppling surfaces are extracted from the sandpile avalanches that appear due to sudden burst of toppling activity in the steady state of these sandpile models. Though a wide distribution of critical flooding heights exists, a critical point is defined by merging the flooding thresholds of all the toppling surfaces. The criticality of the transition is characterized by power-law distribution of island area in the critical regime. A finite size scaling theory is developed and verified by calculating several new critical exponents. The flooding transition is found to be an interesting phase transition and does not belong to the percolation universality class. The universality class of this transition is found to depend on the degree of self-affinity of the toppling surfaces characterized by the Hurst exponent H and the fractal dimension D_f of critical spanning islands. The toppling surfaces of different stochastic sandpile models are found to have a single Hurst exponent, whereas those of different rotational sandpile models have another Hurst exponent. As a consequence, the universality class of different sandpile models remains preserved within the same symmetry of the models.

DOI: 10.1103/PhysRevE.85.031111 PACS number(s): 05.20.−y, 05.65.+b, 68.35.Ct, 64.60.ah

I. INTRODUCTION

Self-affine fractal surfaces often appear in nature as well as in many physiochemical processes [1]. For example: the Earth's relief, mountains [2], clouds [3], etc. in nature, the crack fronts in materials [4], fractured surfaces [5], crumpled paper [6], etc. appeared in different physiochemical processes are found to be self-affine lines or surfaces. The study of percolation process in the topography of synthetically generated self-affine surfaces [7–11] revealed a new type of continuous phase transition with no sharply defined critical point. The technique has recently been applied to characterize fluid flow and conduction in rough surfaces [12], x-ray tomography [13], metal oxide surfaces [14], etc.

Sandpiles are prototypical models for understanding self-organized criticality (SOC) [15], a phenomenon of nonexistence of any characteristic size or time in the nonequilibrium steady state of a class of slowly driven system. During time evolution of these slowly driven systems, if the height of a sand column attains a predefined critical height, a burst of toppling activities occur in the steady state which lead to an avalanche. Once an avalanche is over, a toppling surface corresponding to the avalanche can be defined by the toppling numbers of the lattice sites. Toppling number s_i of a lattice site is the number of times a site is toppled during an avalanche. In continuum, the toppling surface of a sandpile avalanche is possible to describe by a self-affine function of toppling numbers as

$$s(x) \approx \lambda^{-H} s(\lambda x), \tag{1}$$

where λ is a parameter and H is the Hurst exponent of the surface. Recently, the toppling surfaces associated with the avalanches in stochastic (SSM) [16] and rotational (RSM) [17] sandpile models were found to be rough, wrinkled, and self-affine with $H < 0.5$, whereas that of the deterministic Bak, Tang, and Wiesenfeld (BTW) sandpile model [18] was found to be a smooth correlated surface with $H > 0.5$ [19]. This was an added information from the study of toppling surface to the existing results of sandpile models such as BTW, SSM, and RSM belong to different universality classes [17], the SSM and RSM follow finite size scaling (FSS), whereas BTW follows a complicated multiscaling [20], etc. In terms of interface, the toppling dynamics of the Oslo sandpile model was first mapped into growing interface by Paczuski and Boettcher [21], where the height profile of the interface is the accumulated number of toppling. In the context of absorbing state phase transition [22], sandpile models are also described as a growing interface defined by the toppling numbers up to certain time t in a disordered medium [23–25]. The toppling surface defined in Eq. (1) may correspond to one of the final configuration of these growing interfaces in the absorbed state.

In search of further in-depth information hidden in a sandpile avalanche, the toppling surface can be flooded with liquid, say water, and a flooding transition can be studied in the topography of toppling surfaces. During flooding, at each level of water the surface points whose heights are greater than the water level form islands. If the water level is high, there will be a few small islands, whereas if the water level is low, there will be a few small lakes. It is then expected that there exists a critical height at which for the first time water will be able to flood the landscape from one side to the other creating a large number of islands. This is called flooding transition. Interestingly, the study of flooding transition unveils a continuous phase transition at a critical flooding height in the toppling surface topography of stochastic and rotational sandpile models. This is an interesting phenomenon in the literature of sandpile as well as self-organized criticality (SOC) [15]. However, such a transition is not possible in the smooth toppling surface of the BTW sandpile model where at every

*santra@iitg.ernet.in

level of flooding only one island can be extracted. It is then intriguing to characterize the flooding transition in the toppling surface topography of the SSM and the RSM. Since the SSM toppling rule is completely stochastic and the RSM toppling rule is having a rotational symmetry, the toppling surfaces of the SSM and the RSM are entirely different and characterized by different Hurst exponents. The criticality of the flooding transition is found to be determined by the fractal dimension of the critical spanning islands and the degree of self-affinity of the toppling surfaces.

II. FLOODING TRANSITION IN THE TOPPLING SURFACE

The flooding transition is studied in the topography of toppling surfaces of sandpile models of two different classes, SSM [16] and RSM [17]. The toppling rules and extraction of toppling surfaces are described briefly prior to the demonstration of flooding transition in these surfaces. Sandpile models are slowly driven from outside by adding sand grains one at a time and they spontaneously evolve to nonequilibrium steady states without fine tuning of any parameter of the system. During time evolution, if the height of a sand column attains a predefined critical height, a burst of a toppling activity occurs at that column. Due to this intermittent burst, the sand column topples and the sand grains of that column are distributed to its nearest neighbors (NN) following certain toppling rules. As a result, the NN sites may become upper critical and lead to burst of further toppling activities. Consequently, these toppling activities will lead to an avalanche. Toppling surfaces can be generated from these avalanches. During an avalanche the sand columns at different lattice sites topple different number of times. The number of times a site i topples during an avalanche is called the toppling number s_i of that site, a microscopic parameter of the avalanche. The toppling number s_i of each lattice site in an avalanche constitutes a toppling surface of that avalanche. Toppling surfaces are extracted from the large spanning (touching the opposite sides of the lattice) avalanche clusters at the steady states of the RSM and the SSM.

The toppling rules of the RSM and the SSM are now briefly described here on a two dimensional (2D) square lattice of size $L \times L$. Each lattice site i is associated with a nonnegative integer variable h_i, height of the "sand column" at the site i. The system is driven by adding sand grains, one at a time, to randomly chosen lattice sites. As the height h_i of the sand column of a site becomes greater than or equal to h_c, a predefined threshold value, the site become active and bursts into a toppling activity. In a toppling activity, the sand grains of the active site are distributed to its NN sites. For both the RSM and the SSM the critical height is $h_c = 2$. The SSM evolves following a stochastic toppling rule given by $h_i \to h_i - 2$, $h_j \to h_j + 1$, and $j = j1, j2$, where $\{j1, j2\}$ are two randomly selected sites out of four NN sites of the active site i on a square lattice. Thus, the stochasticity in the SSM is imposed by the toppling rules itself. On the other hand, the toppling rules of the RSM are quasideterministic. In this model, two sand grains are given away to two randomly selected NN sites of the active site only on the first toppling. Successive toppling in the RSM occur following a rotational toppling rule given by $h_i \to h_i - 2$, $h_j \to h_j + 1$, and $j = d_i, d_i + 1$, where d_i is the direction from which the last grain was received. If the index j becomes greater than 4 it is taken to be 1. Due to the rotational toppling rule, one sand grain flows in the forward direction, the direction from which the last grain was received, and the other flows in a clockwise rotational direction with respect to the forward direction. Though the rotational toppling rule is deterministic, the direction of the last grain received may change in this model if the toppling sequence is changed and it introduces internal stochasticity into the model. During an avalanche no sand grain is added and the propagation of an avalanche stops if all sites of the lattice become under-critical. The dynamics of both the models are performed with open boundary condition. During an avalanche, the toppling number of a site is stored in an array. The toppling number of a site represents the height of the toppling surface at that point.

Typical toppling surfaces obtained in the RSM and the SSM at their respective steady states are shown in Fig. 1. These surfaces are generated on a 128×128 square lattice. Light brown (light gray) color represents a higher toppling number, whereas dark brown (dark gray) color represents a lower toppling number and the intensity is varied continuously. It can be seen that the toppling surfaces are rough and wrinkled. Entirely different toppling surfaces are obtained due to rotational and stochastic toppling dynamics in the RSM and the SSM, respectively. The SSM toppling surface is highly fluctuating with several large toppling numbers appear randomly here and there. On the other hand, the RSM toppling surface is not totally random as the SSM. The RSM toppling surface is less fluctuating than that of the SSM but consists of several concentric zones of lower toppling numbers centered at large toppling numbers. It can be noted that a BTW toppling surface consists of a single pyramid-like structure where a concentric zone of lower and lower toppling numbers are present around the maximum toppling number without intersection [19]. The RSM toppling surface seems to be consisting of several BTW-type structures around different maximal toppling zones. Due to the internal stochasticity in the RSM, the local correlation in rotational constraint is not able to produce long range correlation generating BTW-like correlated structure.

It should be emphasized here that the toppling surface defined by the toppling number of each lattice site is very different from the surface defined by the height of the sand columns [26,27]. Toppling number s_i keeps more dynamical information than the height h_i of the sand column after the avalanche.

To study the flooding transition, these surfaces are flooded with liquid, say water. At each level of water, the surface points whose heights are greater than the water level form islands. Points belong to the same island are connected by nearest neighbor bonds. At the bottom of the surfaces shown in Fig. 1, the island morphologies at three different levels of flooding are shown. It can be seen that if the water level is high, there appears a few small islands, whereas if the water level is low, a large island appears covering most of the space. At an intermediate level of flooding, there exists a critical height s_c (25 for the RSM and 10 for the SSM) at which a maximum number of islands appear. Below s_c, water is confined locally, whereas above s_c, water is found to be connected from all sides

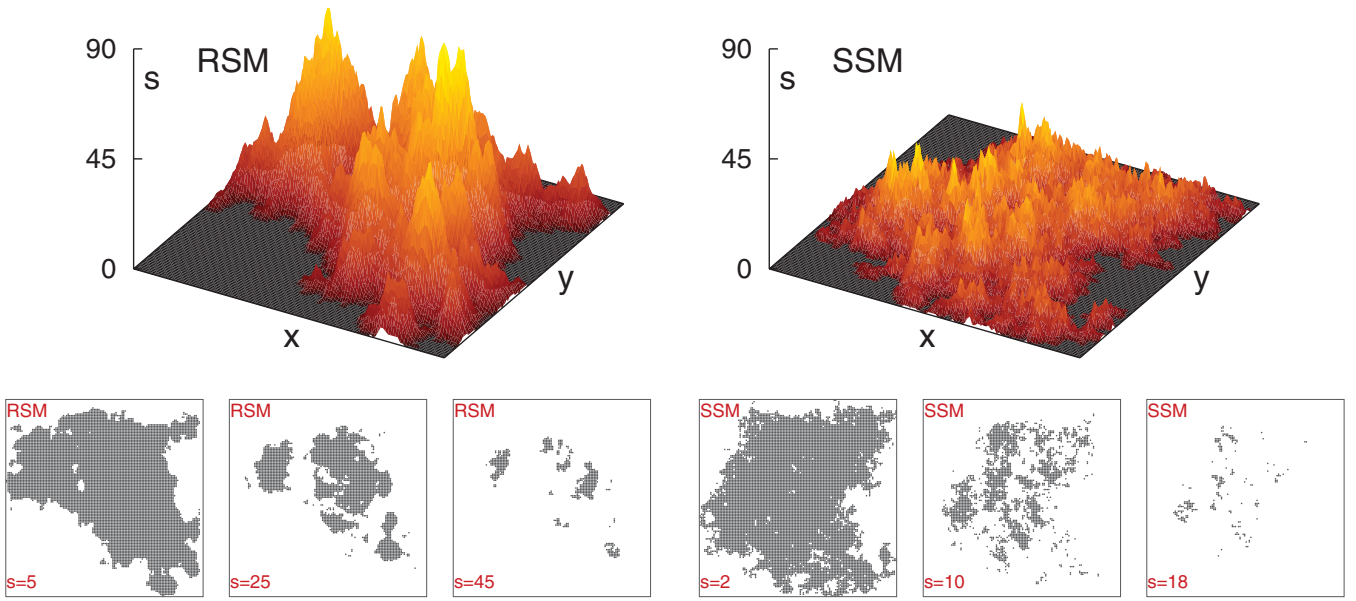

FIG. 1. (Color online) Toppling surfaces generated on a 128 × 128 square lattice for the RSM and the SSM are shown on the top. Islands are shown for three different levels of flooding: $s = 2$, 25, and 45 for the RSM and $s = 2$, 10, and 18 for the SSM. The black dots represent the islands and water is represented by white. Flooding transition occurs at the intermediate level of flooding.

flooding the surface. It is then interesting to study the properties of these islands at the critical transition and verify whether there exits another continuous phase transition through the toppling surface topography which are yields at the steady state of certain dynamical processes. Moreover, it is intriguing to see whether the flooding transition could shine light on the origin of different universality classes of two different sandpile models.

In order to study the flooding transition, extensive computer simulations are performed on 2D square lattices of different sizes L. The system size L varies from 128 to 2048 in multiple of 2. The steady state of the sandpile models is defined as the constant average height of the sand columns. In order to evolve the systems to their respective steady states, first 10^6 avalanches were ignored. At the steady state, 10 configurations were stored for each system size. For a given system, all 10 configurations were evolved further starting with different random number seeds. For each configuration, another 10^5 avalanches were rejected before collecting data. A total of 10^3 toppling surfaces were generated collecting 100 spanning (touching opposite sides of the lattice) avalanche clusters from each starting configuration for each system size L. In order to generate 10^3 spanning avalanche clusters more than 10^7 avalanches were required to generate. The toppling surfaces are then flooded at every height of the surface. At each level of flooding the number of islands appeared is counted and their areas (number of lattice points present in an island) are recorded.

III. FLOODING THRESHOLD

In case of percolation (or generally in continuous phase transitions), the transition occurs at a sharply defined percolation threshold p_c at which the system percolates for the first time if the occupation probability is increased from below p_c [28]. However, in the flooding transition, a wide distribution of the critical height s_c is observed at which the maximum number of islands appear for both the RSM and the SSM. In Fig. 2(a) distribution of the critical heights s_c is plotted for different lattice sizes for the toppling surface of the SSM. It can be noticed that the width of the distribution is increasing with the system size L in contrary to the observation in the usual second order phase transition in which one expects a sharper and sharper distribution with increasing system size. As a consequence, in the $L \to \infty$ limit, there will be critical flooding at all possible heights.

The critical height for flooding is expected to be directly related to the width $W(L)$ of the toppling surface defined as

$$W^2(L) = \left\langle \frac{1}{L^2} \sum_{i=1}^{L^2} (s_i - \bar{s})^2 \right\rangle, \tag{2}$$

where $\bar{s} = \sum_{i=1}^{L^2} s_i / L^2$ is the average height of the surface. The width $W(L)$ is expected to scale with the system size L as

$$W(L) \sim L^{\alpha}, \tag{3}$$

where α is the roughness exponent, similar to that of the saturated width of the growing interfaces in the absorbing state phase transition [25]. The scaling of $W(L)$ of the toppling surfaces with L is shown in Fig. 2(b) and it can be seen that the scaling given in Eq. (3) is satisfied. The exponent α is found as $\alpha = 0.82 \pm 0.03$ for the RSM and 0.73 ± 0.03 for the SSM. It can be noted here that the value of α obtained for the saturated width of the growing interfaces in the absorbing state phase transition for the Manna model is 0.80(3) [23]. The roughness exponent α is known to be related to the exponents describing macroscopic quantity-like toppling size $S = \sum_{i=1}^{L^2} s_i$. The toppling size distribution is given by $P(S,L) = S^{-\tau_s} f_s(S/L^{D_s})$, where τ_s is a critical exponent and D_s is the so-called capacity dimension. As in the case of growing interfaces [21,25], a scaling relation $D_s = 2 + \alpha$ is

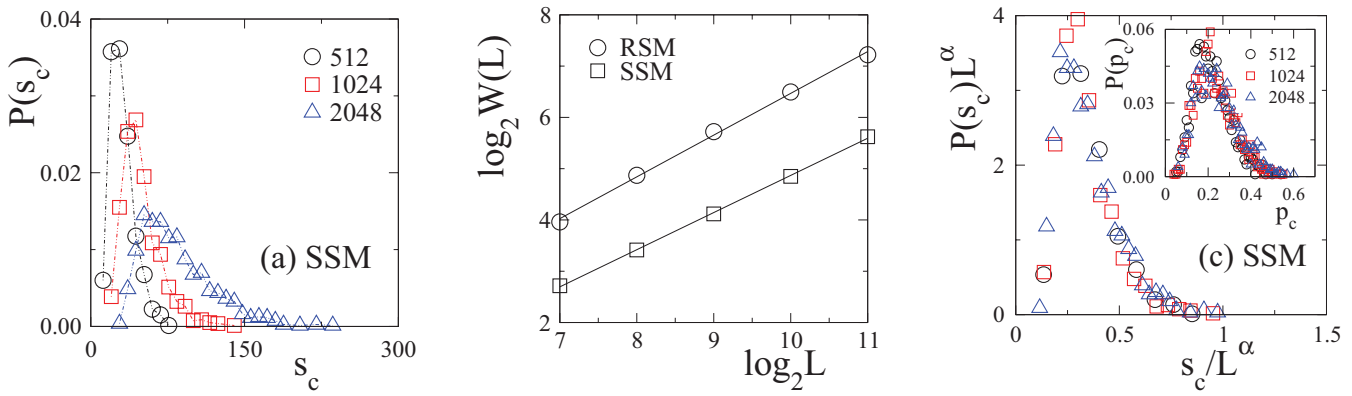

FIG. 2. (Color online) (a) Plot of $P(s_c)$ against s_c for the toppling surface of the SSM for system sizes $L = 512$ (◯), 1024 (□), and 2048 (△). (b) $W(L)$ is plotted against L for the RSM (◯) and the SSM (□). (c) $P(s_c)L^{\alpha}$ is plotted against s_c/L^{α} for the SSM. In the inset, $P(p_c)$ is plotted against the critical area fraction p_c.

expected to be valid in the case of toppling surfaces. For the RSM and the SSM the values of D_s were known to be 2.86 [17] and 2.74 [29], respectively, and thus the above scaling relation is satisfied for both the RSM and the SSM within the error bars. It can be noted that D_s obtained from the roughness exponent ($\alpha \approx 0.8$) measured in Ref. [23] is slightly higher than the measured value for the Manna model.

It is then expected that the critical height s_c should scale with the system size as L^{α}. Since the probability of appearing a critical height decreases with increasing system size, $P(s_c)$ is assumed to scale with the system size as $L^{-\alpha}$. The scaled distribution $P(s_c)L^{\alpha}$ is then plotted against the scaled variable s_c/L^{α} for the SSM taking $\alpha = 0.73$ in Fig. 2(c). A reasonable collapse of data is obtained. A similar data collapse is also obtained for the RSM with $\alpha = 0.82$.

The problem can also be studied in terms of area fraction p, the ratio of the total island area to L^2, as in percolation. It is observed that the critical area fraction p_c also has a wide distribution $P(p_c)$ as shown in the inset of Fig. 2(c). Note that the width of $P(p_c)$ is almost independent of L as it is seen for the scaled distribution $P(s_c)L^{\alpha}$ against the scaled variable s_c/L^{α}. The existence of finite variance in the threshold distribution in the limit $L \to \infty$ was also observed in the contour cuts of self-affine wrinkled surfaces [8,9].

Since there is a wide distribution of critical heights for an ensemble of toppling surfaces, the critical point or the flooding threshold is defined for a given surface as $\Delta s = s - s_c = 0$ and the critical points of all the surfaces are merged together. Data are collected for the same value of Δs of different surfaces and averaging of a physical quantity is made corresponding to the same Δs value. In terms of area fraction, one may define the critical point as $\Delta p = p - p_c = 0$. Though the distribution of critical heights in the RSM and the SSM are different, the critical points of these models are defined identically at $\Delta s = 0$ (or $\Delta p = 0$). The parameter Δs can be considered as a change in the external field in the system with respect to the critical field.

IV. ORDER PARAMETER

In order to identify the order parameter of the flooding transition, one needs to define a spanning island connecting opposite sides of a lattice as in percolation theory. In this transition, such a spanning island appears only at the zero level of flooding. However, there exists a critical flooding level s_c at which maximum number of islands appear. Therefore, a concept of "critical spanning island" is defined as the largest island $a_{\max}(s_c)$ present at the criticality for a given surface. Since for the ensemble of surfaces, the critical point is define by $\Delta s = 0$, the area of the critical spanning island for the ensemble of surfaces is taken as the $\langle a_{\max}(s_c)\rangle$, where $\langle \cdots \rangle$ represents the ensemble average. The order parameter P_{∞} then can be defined as the probability of finding a surface point in an island of area $a \geqslant \langle a_{\max}(s_c)\rangle$ at a given level of flooding. It can be written as

$$P_{\infty} = 1 - P(a), \quad P(a) = \sum_{a}{}' a n_a, \tag{4}$$

where n_a is the number of islands of area a per lattice site at a given Δs, primed sum denotes exclusion of the critical spanning island. P_{∞} is calculated as a function of Δs for three different lattice sizes $L = 512$, 1024, and 2048 for both models. Data for the RSM is plotted in Fig. 3(a). There are two things to notice. First, all the curves are crossing at $\Delta s = 0$ indicating $\Delta s = 0$ as the critical point separating two phases, no flooding and flooding. Second, the plot of P_{∞} becomes flatter and flatter as L is increased rather than sharper and sharper for higher L as expected in a second order phase transition. A similar behavior is also observed for the SSM. However, this is related to the fact that the critical flooding height has wider distribution at a larger L than at a smaller L.

In order to verify the finite size dependence of P_{∞}, a finite size scaling (FSS) analysis has been performed. P_{∞} is assumed as a generalized homogeneous function of Δs and L as given by

$$\lambda P_{\infty} = F[\lambda^a \Delta s, \lambda^b L], \tag{5}$$

where λ is a parameter. Taking $\lambda = L^{-1/b}$, one has

$$P_{\infty} = L^A F[\Delta s/L^B], \tag{6}$$

where $A = 1/b$ and $B = a/b$. Since at $L \to \infty$ limit P_{∞} is expected to be L independent, the FSS function should have a value $(\Delta s/L^B)^{A/B}$ in the same limit. Inserting the value of

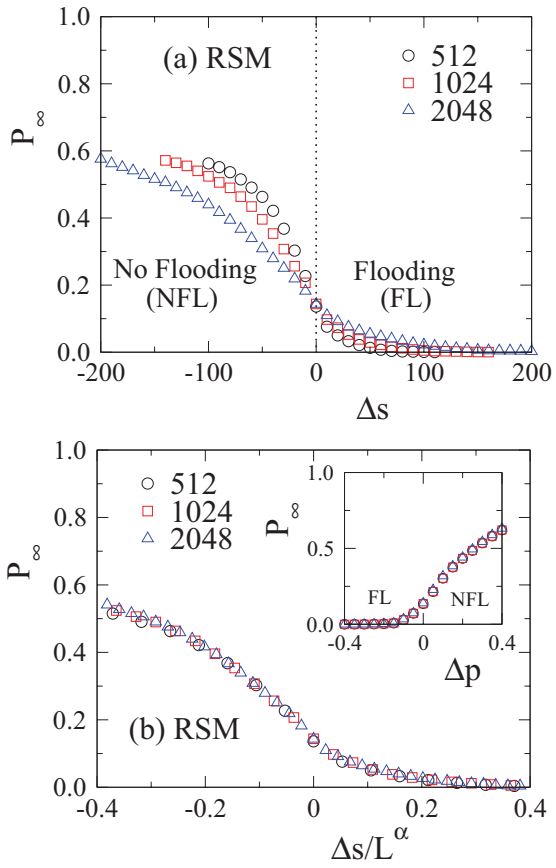

FIG. 3. (Color online) (a) Plot of P_∞ against Δs for the toppling surfaces of the RSM for system sizes $L = 512$ (◯), 1024 (□), and 2048 (△). (b) Plot of P_∞ against the scaled variable $\Delta s/L^\alpha$. In the inset, P_∞ is plotted against $\Delta p = p - p_c$.

$F(\Delta s/L^B)$ in Eq. (6), one has $P_\infty \approx (\Delta s)^{A/B}$. Since Δs is like an external field in the problem, a scaling form for P_∞ with Δs is assumed as

$$P_\infty \approx (\Delta s)^{1/\delta}, \tag{7}$$

where $\delta = B/A$. On the other hand, at $\Delta s = 0$, $P_\infty \approx L^A$ assuming $F(0)$ is a constant. It is also expected that $\Delta s \sim L^\alpha$ as $W(L)$ scales with L. One then has

$$P_\infty \approx (\Delta s)^{A/\alpha}, \quad A/\alpha = 1/\delta. \tag{8}$$

Since $A\delta = \alpha$ and $B = A\delta$, one has $B = \alpha$. At the same time, by definition $P_\infty = L^{(D_f - d)}$, where D_f is the fractal dimension of the critical spanning islands and d is the space dimension. Thus, $A = D_f - d$. Knowing A and B, the FSS form of P_∞ is given by

$$P_\infty = L^{(D_f - d)} F[\Delta s/L^\alpha]. \tag{9}$$

Since the islands here are almost compact, one has $D_f = d = 2$ and consequently it is expected that $P_\infty \approx F[\Delta s/L^\alpha]$. In Fig. 3(b) P_∞ is plotted against the scaled variable $\Delta s/L^\alpha$ taking $\alpha = 0.82$ as for the RSM. A collapse of data is obtained as expected. It not only confirms the scaling theory for P_∞ but also verifies the scaling form of Δs with L. A similar scaling behavior is also obtained for the SSM. In the inset of Fig. 3(b), P_∞ is plotted against $\Delta p = p - p_c$. It can be seen that data for all three L collapse onto a single curve and no rescaling is required. As per percolation theory, the finite size scaling of P_∞ in terms of area fraction is given by $P_\infty = L^{-\beta/\nu} G[\Delta p L^{1/\nu}]$, where β is an order parameter exponent, ν is a correlation length exponent, and $\beta = \nu(d - D_f)$ [28]. Since the argument $\Delta p L^{1/\nu}$ of the scaling function G is found L independent, it seems that the correlation length exponent $\nu \to \infty$. That is also one of the conclusions of the study of synthetic self-affine surfaces [8,11]. As $\nu \to \infty$ and $(d - D_f) \to 0$, then the exponent $\beta = \nu(d - D_f)$ must be finite. One may also note that $A = \alpha/\delta = (D_f - d) \to 0$, then $\delta \to \infty$. Hence, in the $L \to \infty$ limit, as per Eq. (7), the probability of an appearance of a critical spanning island would be uniform at all possible levels of flooding [consistent with Fig. 3(a)]. The order parameter then confirms $\Delta s = 0$ (or $\Delta p = 0$) as a critical point at which no flooding to flooding transition occurs in the topography of the sandpile toppling surfaces.

V. ISLAND AREA DISTRIBUTION

In order to verify the criticality at $\Delta s = 0$ (or $\Delta p = 0$) the probability $P(a_0)$ of appearing on an island of area a_0 in an ensemble of islands collected from all the surfaces at their respective critical heights s_c is determined for a system of size $L = 2048$. In Fig. 4 the distribution $P(a_0)$ is plotted against a_0 in double logarithmic scale for (a) the RSM and (b) the SSM. It can be seen that $P(a_0)$ follows a power-law distribution for both the RSM and the SSM. For a given lattice size L, the island area distribution $P(a_0)$ then should be given by

$$P(a_0) = a_0^{-\eta_0} f_0(a_0/L^{D_f}), \tag{10}$$

where D_f is the fractal dimension of the islands at $\Delta s = 0$ (or $\Delta p = 0$). The best estimate of the exponent η_0 is obtained as 1.81 ± 0.01 for the RSM and 1.90 ± 0.01 for the SSM. The

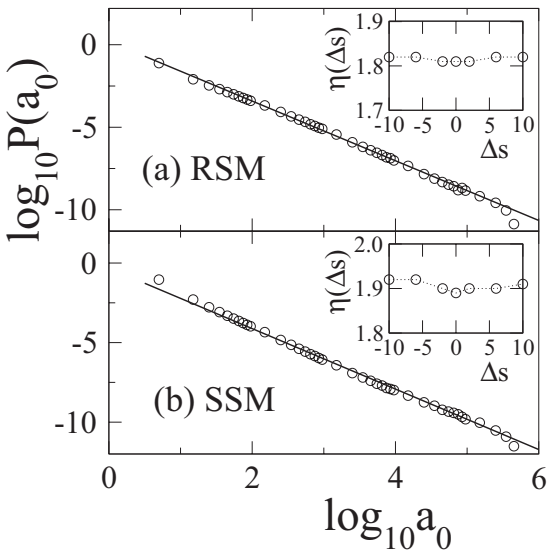

FIG. 4. Plot of island area distribution $P(a_0)$ against a_0 for (a) the RSM and (b) the SSM at $\Delta s = 0$ for the system size $L = 2048$. The solid lines represent the best fitted lines. In the respective insets, $\eta(\Delta s)$ is plotted against Δs for the RSM and the SSM. The exponents are found close to that of η_0.

error bars are the linear least-square-fit errors. It should be noted that η_0 is a new exponent. It is neither equal to the cluster size distribution exponent of percolation $187/91 \approx 2.05$ [28] nor it is equal to the avalanche area distribution exponent τ_a of the respective sandpile models ($\tau_a = 1.334$ for the RSM [17] and $\tau_a = 1.373$ for the SSM [17,30]). These exponents are also different from those recently obtained for the island area distribution at average height of the Kardar-Parisi-Zhang and Edwards-Wilkinson interfaces by Saberi *et al.* [31]. Thus the flooding transition is a continuous phase transition in the topography of the toppling surfaces of stochastic and rotational sandpile models and does not belong to the percolation universality class. However, the flooding transition will be equivalent to a classical percolation transition for uncorrelated surfaces [8,9]. Though the flooding transition is able to characterize the RSM and the SSM distinctly, such a transition does not exist in the smooth toppling surface of the BTW sandpile model [18] for which at every level of flooding a single island will appear. Interestingly, the power-law distribution of island area $P(a)$ is not restricted to $\Delta s = 0$ only rather it is extended over a wide range of Δs. The corresponding exponents $\eta(\Delta s)$ are extracted and plotted against Δs in the respective insets of Fig. 4. The values of $\eta(\Delta s)$s are found close (within error bars) to that of η_0 within $\Delta s = \pm 10$. For large values of Δs (beyond ± 10), the distributions are found to deviate from the critical distribution with different critical exponents. The power-law distribution is observed up to $\Delta s = \pm 100$ on a system of size $L = 2048$. It can be noted here that the area fraction p is ≈ 0.25 corresponding to $\Delta s = 0$ for both the models. Criticality over a wide range of area fraction is also observed in the synthetically generated self-affine surface by Olami [9]. Though the power-law distribution occurs over a wide range of Δs (or Δp), it is observed that the distribution extends for a longest possible range of area in the case of $\Delta s = 0$. This again indicates that $\Delta s = 0$ (or $\Delta p = 0$) is the critical point.

VI. SCALING RELATIONS IN TERMS OF HURST EXPONENT

It is interesting to explore the relationship between the criticality of flooding transition and the self-affinity of toppling surface topography. The self-affinity of a surface is characterized by the Hurst exponent H. The Hurst exponent H of a toppling surface can be determined by measuring directly the correlation between toppling numbers of two sand columns separated by a distance $|\mathbf{r}|$ as well as by obtaining the power spectrum of the toppling number (or height-height) correlation function. The power spectrum technique is applied here to extract the Hurst exponent. The two point height correlation function $C(\mathbf{r})$ is given by

$$C(\mathbf{r}) = \langle |s(\mathbf{x}+\mathbf{r}) - s(\mathbf{x})|^2 \rangle \sim |\mathbf{r}|^{2H}, \tag{11}$$

where $s(\mathbf{x})$ is the toppling number at a position $\mathbf{x}$. The power spectrum of the correlation function is given by

$$S(\mathbf{k}) = \langle |\tilde{s}(\mathbf{k})|^2 \rangle \sim |\mathbf{k}|^{-2(1+H)}, \tag{12}$$

where $\tilde{s}(\mathbf{k}) = \int s(\mathbf{x}) e^{-i\mathbf{k}\cdot\mathbf{x}} dx$ is the Fourier transform of toppling number $s(\mathbf{x})$. The power spectrum $S(\mathbf{k})$ calculated on a system of size $L = 2048$ for both the RSM and the SSM are plotted against $|\mathbf{k}|$ in a double logarithmic scale in Figs. 5(a) and 5(b), respectively. The slopes of the distributions are obtained from linear least-square fit to the data points in the linear region obtained in double logarithmic scale. The Hurst exponents are obtained as: $H(\text{RSM}) = 0.35 \pm 0.01$ and $H(\text{SSM}) = 0.21 \pm 0.01$, consistent with the values of the Hurst exponents obtained from the direct measurement of $C(r)$ as a function of r for a lower lattice size [19]. Since the values of H is less than 0.5, these wrinkled rough toppling surfaces are then self-affine, anticorrelated surfaces. The values of the Hurst exponents then can distinctly characterize stochastic and rotational sandpile models. It can be noted here that the toppling surfaces obtained in the BTW model was found to be a correlated surface with Hurst exponent ≈ 0.66 [19].

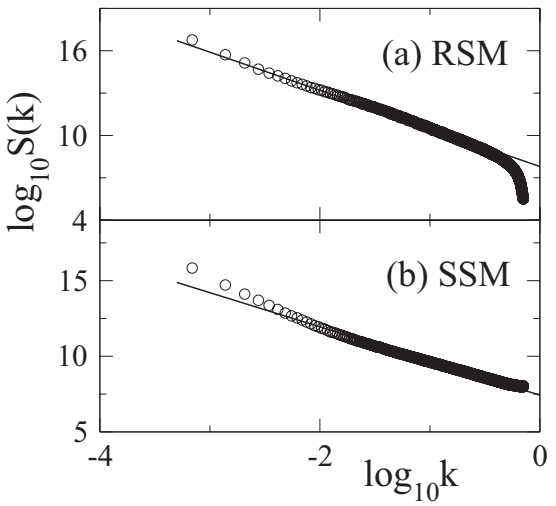

FIG. 5. Power spectral density $S(k)$ against wave number k for toppling surfaces of (a) the RSM and (b) the SSM for a system of size $L = 2048$. Straight lines are the best fitted lines through the data points.

A scaling inequality can now be developed to obtain an upper bound for the critical exponent η_0 in terms of the Hurst exponent H following [9]. The scaling inequality in the critical exponents is developed based on the fact that the number of islands N_0 must be less than the total contour length of all the islands at a given level of flooding. If N_0 is the number of islands at $\Delta s = 0$, the total area of all the islands should be

$$N_0 \int a_0^{-\eta_0+1} f_0(a_0/L^{D_f}) da_0 \approx N_0 L^{D_f(2-\eta_0)}. \tag{13}$$

At the same time, the total island area at $\Delta s = 0$ flooding should also be L^{D_f}, where D_f is the fractal dimension of the islands. The number of islands N_0 then can be obtained as $N_0 = L^{D_f(\eta_0-1)}$. On the other hand, total contour length of all the islands at the criticality should go as L^D, where $D = 2 - H$ is the Mandelbrot exponent [32]. Thus the inequality in island numbers and the contour length can be written as

$$L^{D_f(\eta_0-1)} \leqslant L^{2-H}. \tag{14}$$

The scaling inequality then can be obtained as

$$\eta_0 \leqslant 2 - H/2 \tag{15}$$

assuming $D_f = 2$ for the compact islands. Since $2 - H/2$ is equal to 1.82 ± 0.01 for the RSM and 1.89 ± 0.01 for the SSM, the scaling relation holds as equality for a wide range of Δs (± 10) within error bars. Such scaling equality is also found to be valid for the autocorrelation function for the island areas on self-affine surfaces [33]. The universality class of the flooding transition is thus directly related to the roughness of the toppling surfaces and the fractal dimension of critical spanning islands.

It would now be interesting to obtain the critical exponents describing the macroscopic avalanche properties such as toppling size in terms of H. In order to obtain the macroscopic exponents in terms of H, one needs to obtain the width $W(L)$ of the toppling surface in terms of the two point height correlation function $C(r)$ given in Eq. (11). The square of the width of the toppling surface $W^2(L)$ for a system of size L should be given by $\int_0^L C(r)dr$. Since $C(r) \sim r^{2H}$,

$$W^2(L) \sim L^{1+2H}. \tag{16}$$

Hence, the roughness exponent $\alpha = 1/2 + H$. Since the values of H are 0.35 for the RSM and 0.21 for the SSM, one has $\alpha = 0.85$ and 0.71 for these models, respectively. It can be noted that these values are close to the measured values 0.82 and 0.73, respectively, for the RSM and the SSM as given in Sec. III. The capacity dimension then can be obtained as $D_s = 2 + \alpha = 5/2 + H$. The values of D_s obtained from the Hurst exponent, $D_s = 2.85$ and 2.71 for the RSM and the SSM, respectively, are very close to the measured values of D_s (2.86 [17] and 2.74 [29]) of the respective models. However, such scaling relations seem to be valid for self-affine surfaces with Hurst exponent $H \leqslant 0.5$. For the toppling surfaces with $H > 0.5$, such as the BTW toppling surface with $H \approx 0.66$ [19], D_s would be greater than 3, the expected value [23]. The two point correlation function $C(r)$ for the BTW-type toppling surfaces then should follow the anomalous scaling suggested by Hansen and Mathiesen [34], in which the prefactor to $C(r)$ also has a self-affine character with a different Hurst exponent than H. In this scaling theory, the global Hurst exponent H_g is given by $H_g = H - H_p$, where H_p describes the self-affinity of the prefactor.

VII. FSS ANALYSIS OF ISLAND AREA DISTRIBUTION

A FSS theory is developed by calculating the qth moment $\langle a_0^q \rangle$ of the island area as a function of system size L at $\Delta s = 0$. The qth moment of area distribution is defined as

$$\langle a_0^q \rangle = \int a_0^{-\eta_0+q} f_0(a_0/L^{D_f}) da_0 \sim L^{\sigma_q}, \tag{17}$$

where $\sigma_q = (q + 1 - \eta_0)D_f$. For FSS to be valid, $\sigma_{q+1} - \sigma_q = D_f$ should be satisfied for any q. $\langle a_0^q \rangle$ are calculated excluding the critical spanning islands up to $q = 4$. In Fig. 6 $\langle a_0^q \rangle$ for $q = 1$ and 2 are plotted against L in double logarithmic scale for both models. The values of the exponents are estimated as $\sigma_1 = 0.35 \pm 0.02$ (●) and $\sigma_2 = 2.35 \pm 0.03$ (◯) for the RSM and $\sigma_1 = 0.21 \pm 0.02$ (■) and $\sigma_2 = 2.20 \pm 0.03$ (□) for the SSM by linear least-square fit to the data points. There are a few important things to notice. First, $\sigma_2 - \sigma_1 \approx 2$ for both models. It is also verified for another two higher moments. Thus $P(a_0)$ follows FSS. Second, σ_1 and σ_2 are both

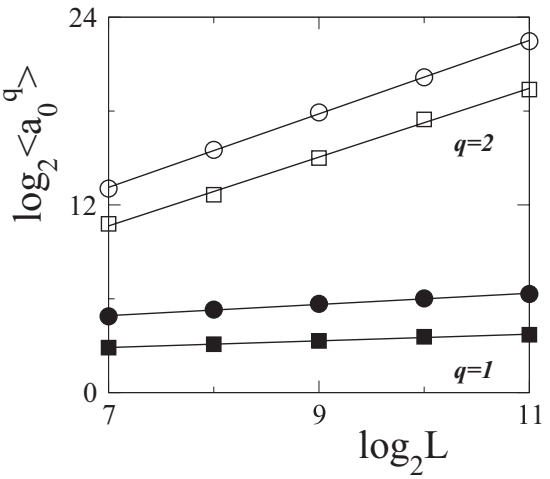

FIG. 6. Plot of $\langle a_0^q \rangle$ against L for the RSM and the SSM for $q = 1$ and 2. Symbols used are: (●) and (◯) for the RSM and (■) and (□) for the SSM. The straight lines are the linear least-square-fit lines.

different for the RSM and the SSM and are then characteristic exponents of these models. Third, the scaling relation $\sigma_q = (q + 1 - \eta_0)D_f$ is satisfied within error bars for both models assuming $D_f = 2$. Fourth, assuming equality in Eq. (15), $\eta_0 = 2 - H/2$ and $D_f = 2$, one has $\sigma_q = 2(q - 1 + H/2)$. Hence, $\sigma_1 = H$ and $\sigma_2 = 2 + H$. It is important to note that the measured values of σ_1 and σ_2 are equal to H and $2 + H$, respectively, for both models. Therefore, all the exponents of flooding transition can be defined in terms of the Hurst exponent H alone taking $D_f = 2$ for the compact islands.

In a continuous phase transition, it is also expected that the fluctuation in island area should diverge at the criticality. The fluctuation in island area $\chi_0(L)$ is defined as

$$\chi_0(L) = \frac{\langle a_0^2(L) \rangle - \langle a_0(L) \rangle^2}{\langle a_0(L) \rangle^2} \tag{18}$$

and it is expected to vary with L as

$$\chi_0(L) \sim L^{\Delta\sigma}, \tag{19}$$

where $\Delta\sigma = \sigma_2 - 2\sigma_1 = 2 - H$. $\chi_0(L)$ is calculated at $\Delta s = 0$ for different L and plotted in Fig. 7. It can be seen that $\chi_0(L)$ follows the scaling law for both the RSM and the SSM with $\Delta\sigma = 1.65 \pm 0.01$ and $\Delta\sigma = 1.78 \pm 0.01$, respectively. The values of $\Delta\sigma$ obtained are also satisfying the scaling relation among σ_2, σ_1, and the Hurst exponent H within the error bars.

FSS form of $\langle a \rangle$ as a function of L and Δp is also verified and it is expected to be

$$\langle a(\Delta p, L) \rangle = L^H g_s(\Delta p L^{1/\nu}), \tag{20}$$

where ν is the correlation length exponent. $\langle a \rangle$ is now estimated for different Δp and L and is plotted in Fig. 8 for the RSM. Interestingly, on one hand the value of $\langle a \rangle$ diverges at $\Delta p = 0$ as expected in a continuous phase transition, on the other hand, the distribution is becoming broader and broader with increasing L in contradiction to a continuous phase transition. In the inset, the scaled average area $\langle a(\Delta p, L) \rangle / L^H$ is plotted against Δp. It can be seen that a good collapse of data is obtained taking $H = 0.35$ for the RSM. Note that Δp

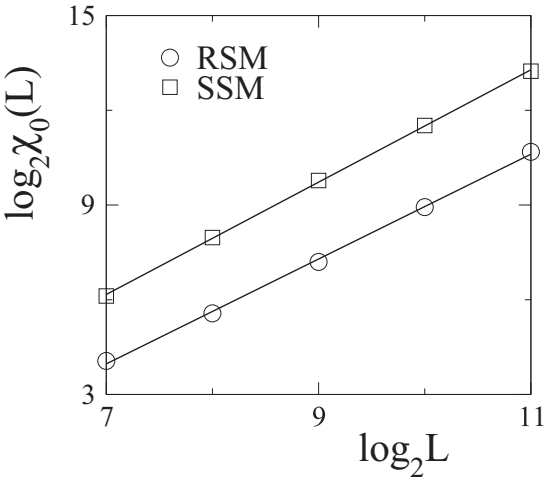

FIG. 7. Plot of $\chi_0(L)$ against L for the RSM (◯) and the SSM (□). The straight lines are the linear least-square-fit lines having slopes 1.65 ± 0.01 and 1.79 ± 0.01 for the RSM and the SSM, respectively.

itself is the scaled variable since $\nu \to \infty$ in this case. A similar collapse of data is also obtained for the SSM with the corresponding values of $H = 0.21$. As per percolation theory, H is also equal to γ/ν, where γ is the critical exponent describing the singularity of $\langle a \rangle$ at $\Delta p = 0$. Since the ratio of γ to ν is finite and $\nu \to \infty$, the exponent γ must be very large. It seems that most of the percolation exponents are infinitely large. But the ratio of these exponents to the correlation length exponent is found to be finite. Therefore, there exists a critical point where the island related quantities will diverge in the $L \to \infty$ limit with appropriate FSS exponents. In that sense, FSS is the most appropriate theory to study this type of phase transition.

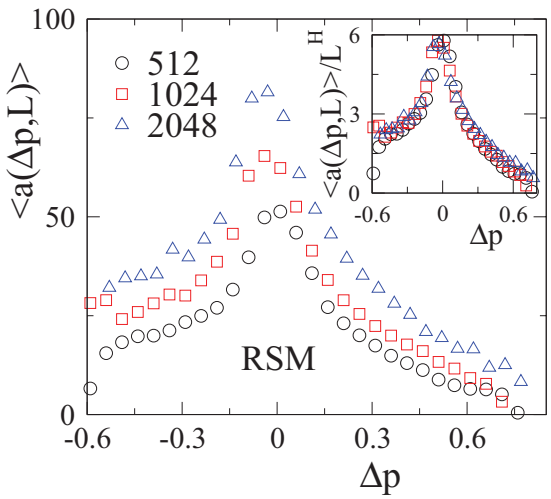

FIG. 8. (Color online) Plot of $\langle a(\Delta p, L) \rangle$ against Δp for $L = 512$ (◯), 1024 (□), and 2048 (△) for the RSM. In the inset, $\langle a(\Delta p, L) \rangle / L^H$ is plotted against Δp for the same set of L. Here Δp itself is a scaled variable as $\nu \to \infty$. A reasonable collapse is observed for $H = 0.35$.

VIII. UNIVERSALITY AND SYMMETRIES OF THE MODELS

In critical phenomena, the universality class of systems in the same spatial dimension is independent of lattice structure or type of interactions and it depends on the symmetry of the order parameter and the number of components present in the order parameter. Interestingly, it was observed that whenever there is an external constraint applied on the equilibrium as well as nonequilibrium lattice statistical models, the universality class of the model has changed. For example, the equilibrium models such as: self-avoiding walk (SAW) [35], directed SAW [36], and spiral SAW [37] belong to different universality classes. Percolation [28], directed percolation [38], spiral percolation [39], and directed-spiral percolation [40] all belong to different universality classes. Similarly for nonequilibrium models, the BTW sandpile model, directed sandpile model [41], the SSM, and the RSM all belong to different universality classes. However, the universality classes of these models remain unaffected even if the details of a model are changed within the same class. For example, different versions of the BTW models [18,42], different SSMs [16,43] or different RSMs [17,44] preserve their own universality classes.

It is seen in the previous section that all the critical exponents of flooding transition can be defined in terms of the Hurst exponent H of the toppling surface and the fractal dimension D_f of islands at the critical flooding. Since the islands are compact and $D_f \approx 2$ for all the models considered here, in order to have the same universality class for all stochastic models the value of H then should be the same for different SSMs and similarly for different rotational models, the Hurst exponent H should be the same for all RSMs. In order to verify such uniqueness of the Hurst exponent of toppling surfaces of sandpile models of the same symmetry, another stochastic model and two other rotational models are considered. The toppling surface of the original Manna model (MSM) [43] is extracted here and the results are compared with the Dhar model. In the original Manna model, all the sand grains are distributed to the nearest neighbors at the time of toppling of an active site, whereas in the Dhar model only two sand grains are distributed randomly to the NNs. Though the original Manna model (MSM) is a nonabelian stochastic model, the Dhar model (SSM) is an abelian stochastic model [16]. Two other rotational sandpile models, the RSM1 and the RSM2 [44], are also considered besides the present RSM considered here. As it is already mentioned in the model section, in the original RSM, the direction of sand flow was decided by the direction of the last sand grain received by the active site. In the RSM1, the direction of sand flow is decided by the direction of the sand grain received by the site to become critical ($h = h_c$) for the first time, whereas in the RSM2, it is decided by the direction of the sand grain received by the site at an arbitrary height on or above the critical height $h \geqslant h_c$ [44]. All these rotational models with broken mirror symmetry are nonabelian. The Hurst exponents of these stochastic and rotational models are determined by measuring the average island area as a function of the system size L at their respective flooding transition point as well as by direct estimation of the power spectrum of two point height correlation function on the largest lattice $L = 2048$. Average

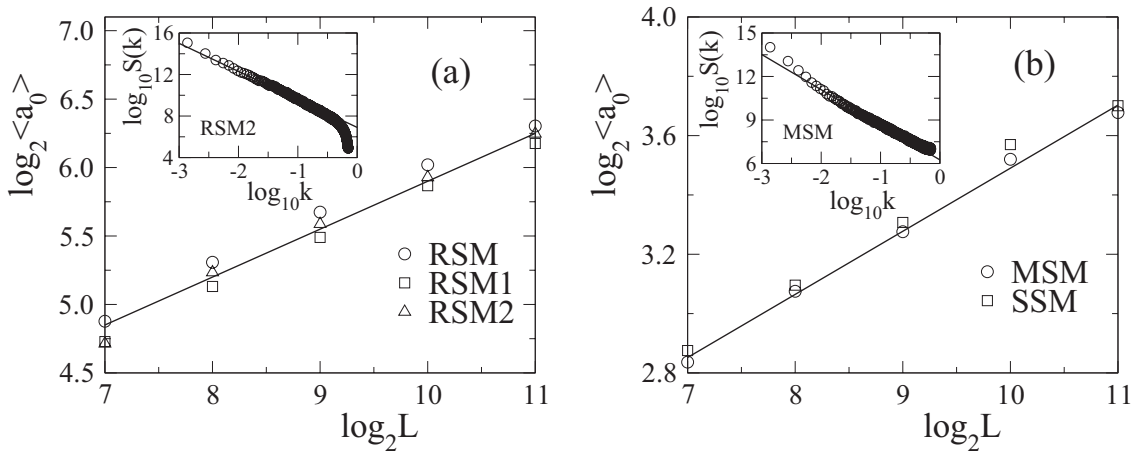

FIG. 9. (a) Plot of $\langle a_0 \rangle$ against L for the RSM, the RSM1, and the RSM2. The solid line has slope 0.35. (b) Plot of $\langle a_0 \rangle$ against L for the MSM and the SSM. The solid line has slope 0.21. In the insets of (a) and (b) $S(k)$ is plotted against k for the RSM2 and the MSM, respectively, for $L = 2048$. The solid lines in the insets are the best fitted lines with slopes 2.70 and 2.42 for the RSM2 and the MSM, respectively.

island area $\langle a \rangle$ at $\Delta s = 0$ for all the rotational models are plotted in Fig. 9(a) and that of the stochastic models (both the SSM and the MSM) are plotted in Fig. 9(b). It can be seen in Fig. 9(a) that all three rotational models are having the same Hurst exponent $H \approx 0.35$ and similarly in Fig. 9(b) the stochastic models are also found to have the same Hurst exponent as $H \approx 0.21$. The values of H are also supported by their respective power spectrum measurements. Plot of $S(\mathbf{k})$ against $|\mathbf{k}|$ for the RSM2 is given in the inset of Fig. 9(a) and that of the MSM is given in the inset of Fig. 9(b). Thus, the values of the Hurst exponents do not depend on the minute details of the toppling dynamics within the same symmetry of the models. Since all the critical exponents related to the flooding transition depend on the Hurst exponent H of the toppling surface and the fractal dimension D_f ($\approx$2) of critical spanning islands, the universality class of flooding transition as well as that of the sandpile models should remain unchanged within the same symmetry of the model. The result is in agreement with a recent conjecture made by Rossi *et al.* [45] in the context of absorbing state phase transitions.

IX. SUMMARY AND CONCLUSION

A continuous phase transition, called flooding transition, is found to occur in the toppling surface topography of stochastic and rotational sandpile models. Such a transition is not possible to occur in the smooth topography of deterministic BTW-type sandpile toppling surfaces. Though there is a wide distribution of flooding thresholds, a critical point is defined by merging the flooding thresholds of all the toppling surfaces. The width of critical height distribution for a given system size is found to scale with the roughness exponent of the toppling surface. The singularity of several island related quantities are explored at the critical point. A number of important observations are noted in the study of flooding transition. An order parameter for the flooding transition is defined in terms of the probability of finding a surface point in the critical spanning island. Power-law distribution of island area is found to exist over a wide range of area fraction. A set of critical exponents are determined. A FSS theory for the island related quantities is developed and verified. Most of the percolation type exponents are found to be infinitely large though their ratios to the correlation length exponent are found finite. The flooding transition is found to be a continuous phase transition and does not belong to the percolation universality class. Not only are the critical exponents of flooding transition obtained in terms of the Hurst exponent H of the toppling surfaces and the fractal dimension D_f of the critical islands, but also the exponents describing the avalanche size distribution are also obtained. The Hurst exponent H is found to be independent of the details of toppling dynamics within the models of the same type of symmetry. For the sandpile models of the same symmetry, the universality class of flooding transition is then determined by the degree of self-affinity of the toppling surfaces if the islands are compact.

ACKNOWLEDGMENT

J. A. Ahmed thanks B. K. Chakrabarti for helpful discussion.

[1] P. Meakin, *Fractals, Scaling and Growth Far From Equilibrium* (Cambridge University Press, Cambridge, 1998).
[2] D. L. Turcotte, *Fractals and Chaos in Geology and Geo-physics* (Cambridge University Press, Cambridge, 1992).
[3] S. Lovejoy, Science **26**, 185 (1982); J. D. Pelletier, Phys. Rev. Lett. **78**, 2672 (1997).
[4] E. Bouchaud, G. Lapasset, and J. Planès, Europhys. Lett. **13**, 73 (1990).
[5] M. J. Alava, P. K. V. V. Nukala, and S. Zapperi, Adv. Phys. **55**, 349 (2006); S. Santucci, M. Grob, R. Toussaint, J. Schmittbuhl, A. Hansen, and K. J. Måløy, Europhys. Lett. **92**, 44001 (2010).

[6] D. L. Blair and A. Kudrolli, Phys. Rev. Lett. **94**, 166107 (2005).
[7] S. V. Buldyrev, S. Havlin, and H. E. Stanley, Physica A **200**, 200 (1993).
[8] J. Schmittbuhl, J.-P. Vilotte, and S. Roux, J. Phys. A **26**, 6115 (1993).
[9] Z. Olami and R. Zeitak, Phys. Rev. Lett. **76**, 247 (1996).
[10] G. Wagner, P. Meakin, J. Feder, and T. Jøssang, Phys. Rev. E **55**, 1698 (1997).
[11] V. V. Mourzenko, J.-F. Thovert, and P. M. Adler, Phys. Rev. E **59**, 4265 (1999).
[12] M. Sahimi, AIChE J. **41**, 229 (1995).
[13] P. Gouze, C. Noiriel, C. Bruderer, D. Loggia, and R. Leprovost, Geophys. Res. Lett. **30**, 1267 (2003).
[14] A. A. Saberi, Appl. Phys. Lett. **97**, 154102 (2010).
[15] H. J. Jensen, *Self-Organized Criticality* (Cambridge University Press, Cambridge, 1998).
[16] D. Dhar, Physica A **270**, 69 (1999).
[17] S. B. Santra, S. Ranjita Chanu, and D. Deb, Phys. Rev. E **75**, 041122 (2007).
[18] P. Bak, C. Tang, and K. Wiesenfeld, Phys. Rev. Lett. **59**, 381 (1987); Phys. Rev. A **38**, 364 (1988).
[19] J. A. Ahmed and S. B. Santra, Europhys. Lett. **90**, 50006 (2010).
[20] S. Lübeck, Phys. Rev. E **61**, 204 (2000); C. Tebaldi, M. De Menech, and A. L. Stella, Phys. Rev. Lett. **83**, 3952 (1999).
[21] M. Paczuski and S. Boettcher, Phys. Rev. Lett. **77**, 111 (1996).
[22] A. Vespignani, R. Dickman, M. A. Muñoz, and S. Zapperi, Phys. Rev. Lett. **81**, 5676 (1998); R. Dickman, A. Vespignani, and S. Zapperi, Phys. Rev. E **57**, 5095 (1998).
[23] A. Vespignani, R. Dickman, M. A. Muñoz, and S. Zapperi, Phys. Rev. E **62**, 4564 (2000).
[24] R. Dickman, M. Alava, M. A. Muñoz, J. Peltola, A. Vespignani, and S. Zapperi, Phys. Rev. E **64**, 056104 (2001); M. Alava and M. A. Muñoz, *ibid.* **65**, 026145 (2002).
[25] M. J. Alava and K. B. Lauritsen, Europhys. Lett. **53**, 563 (2001); M. Alava, J. Phys. Condens. Matter **14**, 2353 (2002).
[26] J. Krug, J. E. S. Socolar, and G. Grinstein, Phys. Rev. A **46**, R4479 (1992).
[27] J. G. Oliveira, J. F. F. Mendes, and G. Tripathy, Phys. Rev. E **69**, 031105 (2004).
[28] D. Stauffer and A. Aharony, *Introduction to Percolation Theory*, 2nd ed. (Taylor and Francis, London, 1994).
[29] A. Chessa, H. E. Stanley, A. Vespignani, and S. Zapperi, Phys. Rev. E **59**, R12 (1999).
[30] K. Christensen and Z. Olami, Phys. Rev. E **48**, 3361 (1993); A. Ben-Hur and O. Biham, *ibid.* **53**, R1317 (1996); S. Lübeck and K. D. Usadel, *ibid.* **55**, 4095 (1997).
[31] A. A. Saberi, M. D. Niry, S. M. Fazeli, M. R. Rahimi Tabar, and S. Rouhani, Phys. Rev. E **77**, 051607 (2008).
[32] B. B. Mandelbrot, *The Fractal Geometry of Nature* (Freeman, New York, 1992).
[33] S. B. Ramisetti, C. Campañá, G. Anciaux, J. F. Molinari, M. H. Müser, and M. O. Robbins, J. Phys. Condens. Matter **23**, 215004 (2011).
[34] A. Hansen and J. Mathiesen, in *Modeling Critical and Catastrophic Phenomena in Geoscience: A Statistical Physics Approach*, edited by P. Bhattacharyya and B. K. Chakrabarti, Lecture Notes in Physics, Vol. 705 (Springer, Berlin, 2006), pp. 93–110.
[35] P. G. de Gennes, *Scaling Concepts in Polymer Physics* (Cornell University Press, Ithaca, NY, 1979).
[36] B. K. Chakrabarti and S. S. Manna, J. Phys. A **16**, L113 (1983); S. Redner and I. Majid, *ibid.* **16**, L307 (1983).
[37] H. J. W. Blöte and H. J. Hilhorst, J. Phys. A **17**, L111 (1984); K. Y. Lin, *ibid.* **18**, L145 (1985).
[38] H. Hinrichsen, Adv. Phys. **49**, 815 (2000), and references therein.
[39] S. B. Santra and I. Bose, J. Phys. A **24**, 2367 (1991), and references therein.
[40] S. Sinha and S. B. Santra, Eur. Phys. J. B **39**, 513 (2004), and references therein.
[41] D. Dhar and R. Ramaswamy, Phys. Rev. Lett. **63**, 1659 (1989).
[42] S. Lübeck, Phys. Rev. E **56**, 1590 (1997); O. Biham, E. Milshtein, and O. Malcai, *ibid.* **63**, 061309 (2001).
[43] S. S. Manna, J. Phys. A **24**, L363 (1991).
[44] J. A. Ahmed and S. B. Santra, Eur. Phys. J. B **76**, 13 (2010).
[45] M. Rossi, R. Pastor-Satorras, and A. Vespignani, Phys. Rev. Lett. **85**, 1803 (2000).